Skeletal Radiology (2019) 48:1221–1231
https://doi.org/10.1007/s00256-019-3151-5

SCIENTIFIC ARTICLE

Anatomical variations related to pathological conditions of the peroneal tendon: evaluation of ankle MRI with a 3D SPACE sequence in symptomatic patients

Elif Ersoz[1] · Nil Tokgoz[1] · Ahmet Y. Kaptan[2] · Akif M. Ozturk[2] · Murat Ucar[1]

Received: 30 August 2018 / Revised: 18 December 2018 / Accepted: 7 January 2019 / Published online: 6 February 2019

Abstract

Objective To evaluate anatomical variations in the lateral ankle and their relationships with pathological conditions of the peroneal tendon on magnetic resonance imaging (MRI) in symptomatic patients.

Materials and methods Sixty-nine ankles MRIs of 60 adult patients with symptomatic ankles were included. The presence and sizes of peroneal tubercle and retrotrochlear eminence (RTE), the prevalence of peroneus quartus (PQ), os peroneum, and boomerang-shaped peroneus brevis (PB) tendon, the shape of the retromalleolar fibular groove (RMFG), and the location of the PB muscle–tendon junction were evaluated. The relationships of these variations with peroneal tendinopathies were assessed. The correlations between pathological peroneal conditions on MRI and clinical findings were evaluated.

Results Peroneal tubercle (mean size, 3.2 mm) and RTE (mean size, 4.5 mm) were identified in 58 (84%) and 69 (100%) ankles respectively. PQ muscle, os peroneum, and boomerang-shaped PB tendon were found in 9 (13%), 7 (10%), and 24 (34.8%) ankles respectively. The RMFG was concave, flat, convex, and irregular in 14 (20.3%), 40 (58%), 13 (18.8%), and 2 (2.9%) ankles respectively. Sixteen (23.2%) patients had low-lying PB muscle belly. Only boomerang-shaped PB tendons showed a significant relationship with peroneal tendinopathies. MRI and clinical findings had a poor correlation in pathological peroneal conditions and both had low sensitivity in diagnosis.

Conclusion Lateral ankle anatomical variations are common and cannot be attributed to pathological conditions of the peroneal tendon, except for boomerang-shaped PB tendons. Both clinical and MRI findings have low sensitivity in the diagnosis of peroneal tendinopathies, which are often incidental findings on MRI.

Keywords Magnetic resonance imaging · Ankle · Foot · Pathological conditions of the peroneal tendon · Anatomical variations

Introduction

Laterally, peroneal tendons, which function as primary evertors of the ankle, are dynamic stabilizers of the joint. The superior peroneal retinaculum (SPR) is also an important stabilizer because it keeps these tendons in the peroneal groove. The close relationship between the peroneal tendons and SPR in concomitant diseases complicate the clinical diagnosis and treatment of lateral ankle pain [1]. Although most pathological conditions of the peroneal tendon are caused by acute trauma or chronic overuse, some foot–ankle anatomical variations have been suggested to be predisposing factors for peroneal tendon injuries [2–10]. Magnetic resonance imaging (MRI) is very important in the diagnosis of ankle disorders and has been used in studies to show lateral ankle variants and pathological peroneal tendons. Studies have used conventional MRI sequences and included asymptomatic patients.

It has been reported that peroneal tendinopathies are not uncommon on MRI in asymptomatic patients [11, 12]. To our knowledge, there are no detailed studies revealing lateral ankle variations in detail with three-dimensional (3D) MRI sequences and evaluating their relationship with pathological peroneal tendons in symptomatic patients, as assessed using a standard clinical scoring system. Thus, the primary purpose of

✉ Elif Ersoz
eliffersz@gmail.com

[1] Department of Radiology, Gazi University Faculty of Medicine, Ankara, Turkey

[2] Department of Orthopedics and Traumatology, Gazi University Faculty of Medicine, Ankara, Turkey

the present retrospective study was to reveal anatomical variations of the lateral ankle by means of both conventional and 3D T1-weighted (T1W) sampling perfection with application-optimized contrasts using different flip-angle evolution (SPACE) sequences, and to assess the relationships of these variants with patient demographics (age and sex) and pathological peroneal tendons in symptomatic patients, as evaluated using a standard clinical scoring system. We also demonstrated the associated MRI findings (SPR injury, soft-tissue edema, and peroneal tenosynovitis) with peroneal tendinopathies and investigated the correlations between MRI and clinical findings in the diagnosis of pathological conditions of the peroneal tendon.

Materials and methods

Institutional review board approval was granted for the study, and informed consent was obtained from each patient.

Patients

Seventy-eight ankle MRIs of 67 patients who were referred by the same two orthopedic surgeons (A.M.O., A.Y.K.) were obtained in our radiology department between 1 March 2016, and 30 November 2016. All patients had presented to hospital because of ankle pain. Patients with a history of ankle trauma within the last 2 years (including ankle sprain), surgery, tumor, infection, and arthritis were excluded from the study. MRI examinations of inadequate quality were also excluded.

Magnetic resonance imaging of 69 ankles in 60 patients (46 women, 14 men) met the inclusion criteria were included in this study. The mean age of the patients was 42 (range, 18–70) years.

Clinical evaluation

All patients were evaluated according to the American Orthopedic Foot and Ankle Society (AOFAS) scoring system by the same orthopedic surgeons before MRI examinations (Table 1). In this clinical examination, peroneal tenderness and peroneal instability were noted.

MR imaging protocol

Thirty-six of the 69 (52%) MRIs were performed using a 3-Tesla (T) system (Magnetom Verio syngo MR B17; Siemens, Erlangen, Germany) with a 12-channel head coil, and 33 MRIs (48%) were performed using a 1.5-T system (Magnetom Aera E11; Siemens Erlangen, Germany) with a 16-channel extremity coil. The duration of the MRI examination was between 20 and 25 min. Subjects were examined in the supine position with a 90° angle between the leg and the foot. We used pillows to stabilize the ankle in the extremity and head coils.

On the 3-T MRI system, T1W spin-echo (SE) images were obtained in the sagittal (repetition time [TR] ms/echo time

Table 1 American Orthopedic Foot and Ankle Society score

Ankle–hindfoot scale (100 points total)	
Pain (40 points)	
None	40
Mild, occasional	30
Moderate, daily	20
Severe, almost always present	0
Function (50 points)	
Activity limitations, support requirement	
No limitations, no support	10
No limitation of daily activities, limitation of recreational activities, no support	7
Limited daily and recreational activities, cane	4
Severe limitation of daily and recreational activities, walker, crutches, wheelchair, brace	0
Maximum walking distance, blocks	
Greater than 6	5
4–6	4
1–3	2
Less than 1	0
Walking surfaces	
No difficulty on any surface	5
Some difficulty on uneven terrain, stairs, inclines, ladders	3
Severe difficulty on uneven terrain, stairs, inclines, ladders	0
Gait abnormality	
None, slight	8
Obvious	4
Marked	0
Sagittal motion (flexion plus extension)	
Normal or mild restriction (30° or more)	8
Moderate restriction (15–29°)	4
Severe restriction (less than 15°)	0
Hindfoot motion (inversion plus eversion)	
Normal or mild restriction (75–100% normal)	6
Moderate restriction (25–74% normal)	3
Marked restriction (less than 25% normal)	0
Ankle–hindfoot stability (anteroposterior, varus–valgus)	
Stable	8
Definitely unstable	0
Alignment (10 points)	
Good, plantigrade foot, midfoot well aligned	10
Fair, plantigrade foot, same degree of midfoot malalignment observed, no symptoms	8
Poor, nonplantigrade foot, severe malalignment, symptoms	0
Total	100

[TE] ms, 700/19; section thickness, 3 mm; field of view (FOV), 180 mm; matrix size, 358 × 448) and axial (TR/TE, 600/19; section thickness, 4 mm; FOV, 180 mm; matrix size, 293 × 448) planes. Fat-suppressed FSE T2-weighted (T2W) images were obtained in the coronal (TR/TE, 3,200/92; section thickness, 4 mm; FOV, 180 mm; matrix size, 358 × 448) and axial (TR/TE, 4,650/89; section thickness, 4 mm; FOV, 180 mm; matrix size, 198 × 320) planes. Short tau inversion recovery (STIR) (TR/TE, 3,700/52; inversion time (TI), 220 ms; section thickness, 3 mm; FOV, 180 mm; matrix size, 269 × 384) and 3D T1W SPACE (TR/TE, 400/21; section thickness, 0.7 mm; FOV, 180 mm; matrix size, 256 × 256) sequences were performed in the sagittal plane.

On the 1.5-T MRI system, T1W SE images were obtained in the sagittal (TR/TE, 376/12; section thickness, 4 mm; FOV, 160 mm; matrix size, 269 × 384) and axial (TR/TE, 413/12; section thickness, 3 mm; FOV, 150 mm; matrix size, 234 × 384) planes. Fat-suppressed FSE T2W images were obtained in the coronal (TR/TE, 4,000/93; section thickness, 4 mm; FOV, 150 mm; matrix size, 224 × 320) and axial (TR/TE, 3,660/109; section thickness, 3 mm; FOV, 150 mm; matrix size, 182 × 320) planes. STIR (TR/TE, 5,070/69; TI, 140 ms; section thickness, 4 mm; FOV, 160 mm; matrix size, 179 × 256) and 3D T1W SPACE (TR/TE, 400/21; section thickness, 0.7 mm; FOV, 180 mm; matrix size, 256 × 256) sequences were performed in the sagittal planes. Fat-suppressed proton density (PD)-weighted sequence (TR/TE, 2,850/26; section thickness, 4 mm; FOV, 150 mm; matrix size, 224 × 320) was obtained in the coronal plane.

Analysis of MR images

Magnetic resonance images were read in consensus by an experienced musculoskeletal radiologist (NT, 20 years' experience in musculoskeletal radiology) and a radiology resident (EE, 14 months' experience in musculoskeletal radiology) who were unaware of the clinical findings. 3D T1W SPACE sequences provided volume imaging to reconstruct the images in multiple arbitrary planes for bone, tendon, and ligament assessment.

The shape of the retromalleolar fibular groove (RMFG) was assessed on axial images 1 cm proximal to the fibular tip. The RMFG was described according to the study by Wang et al. and classified as concave, flat, convex, or irregularly contoured [1].

The presence of the peroneal tubercle and retrotrochlear eminence (RTE) was evaluated on reformatted axial images obtained from sagittal 3D T1W SPACE sequences. The peroneal tubercle and RTE are defined as the anterior and posterior prominences in the lateral aspect of the calcaneus respectively. The sizes of both prominences were measured as the maximal distance between the apex and reference line along the lateral cortex of the calcaneus, similar to the study by Saupe et al. [10]. If the size were more than 5 mm, it was defined as a hypertrophic prominence, similar to that used in the same study [10].

The distance of the peroneus brevis (PB) musculotendinous junction (MTJ) from the fibular tip was measured on sagittal 3D T1W SPACE sequences. The MTJ was described as the site where the muscle belly was not seen when followed from its proximal portion [10]. Positive and negative values were defined as the PB MTJ situated distal and proximal to the fibular tip respectively. A low-lying peroneus muscle belly was defined for positive values. The angle between the plantar fascia and the longitudinal axis of the tibia was measured in a manner similar to that described in the study by Saupe et al., because a relationship between dorsiflexed foot position and MTJ distal extension on MRI was reported in the study by Rademaker et al. [10, 13].

The presence of an os peroneum was defined as an accessory bone located close to the calcaneocuboid joint within the peroneus longus (PL) tendon. If the os peroneum were present, the bone marrow edema, fracture or multipartite appearance of this structure was also noted.

The presence of an accessory peroneus quartus (PQ) muscle was noted if an accessory muscle and tendon were located medial and posterior to the peroneal tendons and separated by a fat plane. As there are variable insertions (such as calcaneus, cuboid bone, PL tendon) for this accessory muscle, its insertion site was also defined.

The shape of the PB tendon was evaluated in the axial plane. The tendon of the PB is located anteromedial to the PL tendon and normally appears flat or mildly crescentic. If the central part of the PB tendon is thinner and the PL tendon is partially surrounded by it, the PB tendon is defined as "boomerang-shaped." The normal insertion sites of peroneal tendons are defined as: the lateral aspect of the fifth metatarsal base for the PB and the plantar posterolateral aspect of the medial cuneiform and the lateral side of the first metatarsal base for PL tendons. Normal peroneal tendons are located medial to the lateral fibular margin [1]. Insertional variations of peroneal tendons were noted.

The peroneal tendons were evaluated on MRI and classified into five groups:

1. Normal (uniform low signal intensity within the tendons on all pulse sequences)
2. Tendinosis (homogeneously increased signal intensity within tendons)
3. Partial tear (partial-thickness discontinuity of the tendons and fluid signal intensity on axial fat-suppressed T2W sequence)
4. Full-thickness tear (complete disruption of tendon fibers with fluid signal intensity inside confirmed in more than one imaging plane)
5. Longitudinal split-tear (longitudinal disruption of tendon fibers with two discrete hemitendons on coronal fat-suppressed T2W and/or PDW sequences)

In the absence of morphological changes, the increase in signal intensity of peroneal tendons in their curved portions (around the lateral malleolus) on short TE (T1W) sequences and the decrease or absence of this signal on longer TE (T2W) sequences was defined as the "magic angle" phenomenon. This criterion was used to differentiate the magic angle phenomenon from a pathological signal increase due to tendinosis. Dislocations of peroneal tendons were evaluated.

Superior peroneal retinaculum injury (stripping of the periosteal attachment of the distal fibula or tear), lateral ankle soft-tissue edema, synovial effusion, and thickening of the peroneal tendon sheath were also recorded.

Statistical analysis

All analyses were performed using Statistical Package for the Social Sciences (SPSS) software, version 20. Descriptive statistical methods (frequency and percentage, average, and standard deviation) were used for the evaluation of the variations and shown as histograms. Medians, ranges, and 10th and 90th percentiles of the peroneal tubercle and RTE and the position of the PB MTJ were calculated. The Mann–Whitney *U* test was used to compare the mean values of the quantitative data according to independent groups. Pearson's Chi-squared test, Yates's correction test, and Fisher's exact test were used to compare qualitative data. Sensitivity, specificity, positive predictive, negative predictive, and accuracy values of MRI and clinical examination findings were investigated in pathological conditions of the peroneal tendon.

A p value < 0.05 was considered to indicate a statistically significant difference with 95% confidence intervals.

Results

Sixty-nine ankle MR examinations in 60 symptomatic patients (46 women, 14 men) were included in this study. The mean age of the patients was 42 (range, 18–70) years (Table 2).

Table 2 Patient demographics

Demographic	Value (%)
MRI scans	
1.5 T	36 (52.00)
3 T	33 (48.00)
Age	41.86 ± 14.25
Gender	
Male	14 (23.40)
Female	46 (76.60)
Injury side	
Left	39 (56.00)
Right	30 (43.50)

Anatomical variations of MRI

The RMFG was concave in 14 (20.3%), flat in 40 (58%), convex in 13 (18.8%), and irregular in 2 (2.9%) ankles. There were flat, convex or irregular fibular grooves in 79.7% of the ankles. A statistically significant correlation was found between female sex and flat-shaped RMFGs ($p < 0.05$).

The peroneal tubercle and RTE were identified in 58 (84%) and 69 (100%) out of 69 ankles respectively (Figs. 1, 2). The median size of the peroneal tubercle was 3.2 (range, 1.2–9.2) mm. The median size of the RTE was 4.5 (range, 1.7–8.4) mm. The peroneal tubercle and RTE were hypertrophic (>5 mm) in 10% and 32% of ankles respectively.

Fig. 1 A 29-year–old female patient with lateral ankle pain. Axial T1-weighted (T1W) magnetic resonance images (MRI) demonstrating hypertrophic peroneal tubercle (>5 mm). The peroneus brevis (PB) and peroneus longus (PL) tendons are located anterior (*arrowhead*) and posterior (*curved arrow*) to the peroneal tubercle (arrow) respectively

Fig. 2 A 35-year-old man with lateral ankle pain. Axial 3D T1W sampling perfection with application-optimized contrasts using different flip-angle evolution (SPACE) MRI showing retrotrochlear eminence (*arrow*) posterior to the PL tendon

The MTJ of the PB muscle was located within a range between 30.6 mm proximal and 11.2 mm distal to the fibular tip (median, 4.7 mm proximal to the fibular tip). A low-lying peroneus muscle belly was found in 16 (23.2%) ankles, in which the MTJ of the PB muscle was distal to the fibular tip.

The 10th, 50th, and 90th percentiles and range values are presented in Table 3.

The mean angle between the plantar fascia and the longitudinal axis of the tibia was 97.8° (range, 79–127°). No significant correlation was found between the foot position angle and the location of the MTJ of the PB muscle.

Seven patients had os peroneum, which was bilateral in two patients (Fig. 3). Accordingly, there were 9 (13%) ankles with os peroneum. All patients with os peroneum were female. There was no bone marrow edema, fracture or multipartite appearance of the os peroneum in these cases.

The PQ muscle was found in 2 male and 6 female patients (Fig. 4). A female patient had accessory PQ muscles bilaterally. Accordingly, there were 9 (13%) ankles with accessory PQ muscles. The insertions for these accessory muscles were calcaneus (peroneocalcaneus externum) in 8 (89%) ankles and the PL tendon (peroneoperoneolongus) in one ankle (11%).

There were 6 male and 17 female patients with boomerang-shaped PB tendons. A female patient had bilateral boomerang-shaped PB tendons. Accordingly, this variation was found in 24 ankles (34.8%; Fig. 5).

Except for the shape of the RMFG and os peroneum, no ankle anatomical variations showed a relationship with sex ($p > 0.05$). There was no relationship between these variants and the age of the patients.

Pathological peroneal tendon on MRI

The PB tendon was intact on MRI in 54 (78.3%) ankles. There was tendinosis in 7 (10.1%), a partial tear in 1 (1.5%), and a longitudinal split tear in 7 (10.1%) out of 69 ankles. None of the patients had full-thickness tears of the PB tendon. On MRI, the PL tendon was intact in 55 (79.7%) 69 ankles. There was tendinosis in 13 (18.8%) ankles and a longitudinal split tear in 1 (1.5%) out of 69 ankles. None of the patients had partial or full-thickness tears of the PL tendon. A female patient had longitudinal split tears of both PB and PL tendons (Fig. 6). There were no patients with MRI findings of dislocations or insertional variations of peroneal tendons. No significant correlations were found between peroneal pathological conditions and age or sex.

There was no relationship between the shape of the RMFG and pathological peroneal tendons ($p > 0.05$). The sizes of the peroneal tubercles and RTEs showed no statistically significant correlation with pathological peroneal tendons ($p > 0.05$). Also, the location of the PB MTJ and the presence of the os peroneum or accessory PQ muscle revealed no significant associations with peroneal tendinopathies ($p > 0.05$).

Table 3 Medians, ranges, and 10th and 90th percentiles of the peroneal tubercle, the retrotrochlear eminence, and the position of the peroneus brevis musculotendinous junction

Anatomical parameter	*n*	10th percentile (mm)	50th percentile (mm)	90th percentile (mm)	Range (mm)
Peroneal tubercle	58	1.8	2.8	5.5	1.2 to 9.2
Retrotrochlear eminence	69	3.1	4.3	6.2	1.7 to 8.4
Position of the peroneus brevis MTJ	69	−15.1	−6	+6.1	−30.6 to +11.2

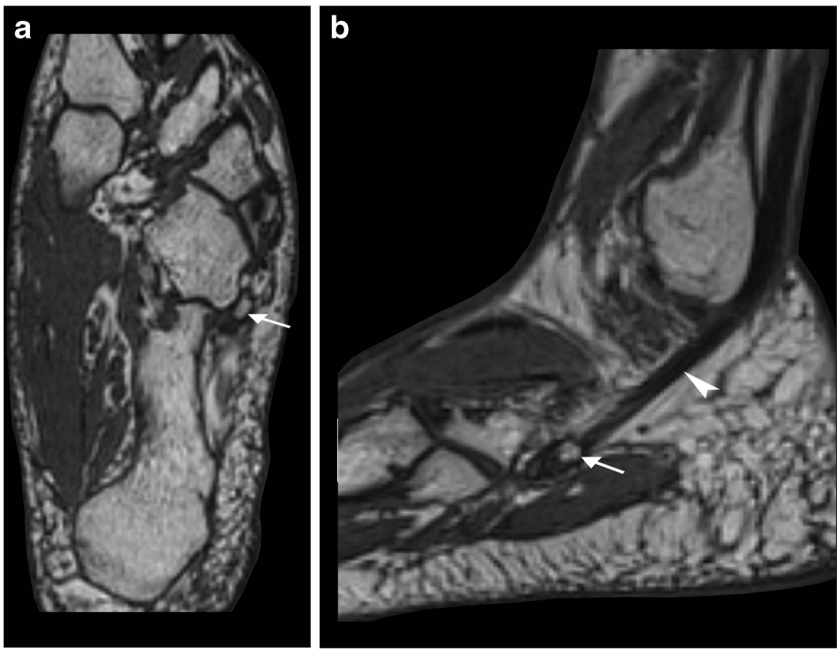

Fig. 3 **a** Axial and **b** sagittal T1W MR images of a 35-year-old female patient with lateral ankle pain. The os peroneum (*arrow*) is located at the lateral plantar aspect of the cuboid bone (**a, b**) and within the substance of PL tendon (*arrowhead*; **b**)

A statistically significant correlation was found between boomerang-shaped PB tendons and both PB and PL tendinosis ($p < 0.05$). There was also a significant correlation between boomerang-shaped tendons and both PB and PL tendon tears ($p < 0.05$). There was no relationship between RMFG shape and boomerang-shaped PB tendons ($p > 0.05$).

The prevalence values of anatomical variations and pathological peroneal tendons are presented in Table 4.

Additional pathological conditions of the lateral ankle on MRI

Superior peroneal retinaculum injury and lateral ankle soft-tissue edema were found in 6 (8.7%) and 29 (42%) ankles respectively. Synovial effusion and thickening of the peroneal tendon sheath were found in 24 (34.8%) and 7 (10.1%) ankles respectively.

Magnetic resonance imaging findings of lateral ankle soft-tissue edema showed statistically significant correlations with pathological conditions of both the PB and the PL tendon ($p < 0.05$). A significant correlation was found between boomerang-shaped PB tendons and soft-tissue edema of lateral ankles ($p < 0.05$). There was also a correlation between boomerang-shaped PB tendons and synovial thickening of peroneal tendon sheaths ($p < 0.05$). Correlations among anatomical variants, additional pathological findings, and pathological conditions of the peroneal tendon are presented in Table 5.

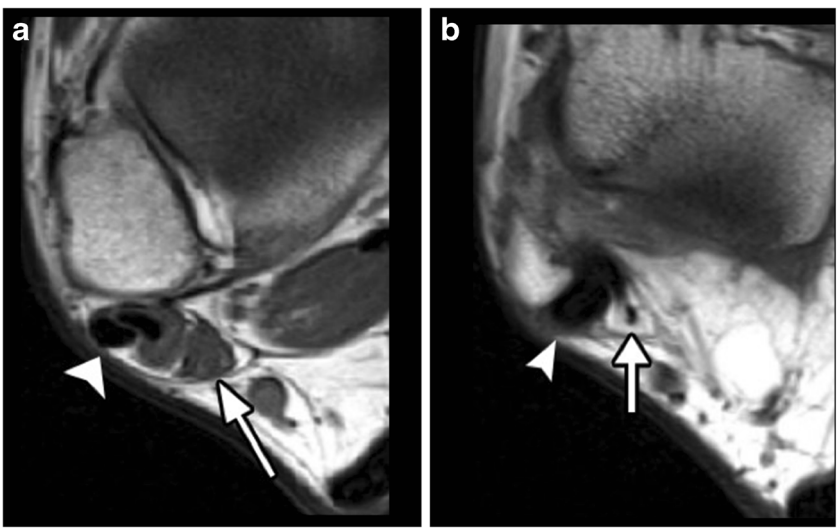

Fig. 4 T1W MRI of a 27-year-old man with lateral ankle pain. **a** The peroneus quartus muscle (*arrow*) and **b** its tendon (*arrow*) are located posteromedial to the peroneal tendons (*arrowhead*) (**a, b**) and separated from them by a fat plane

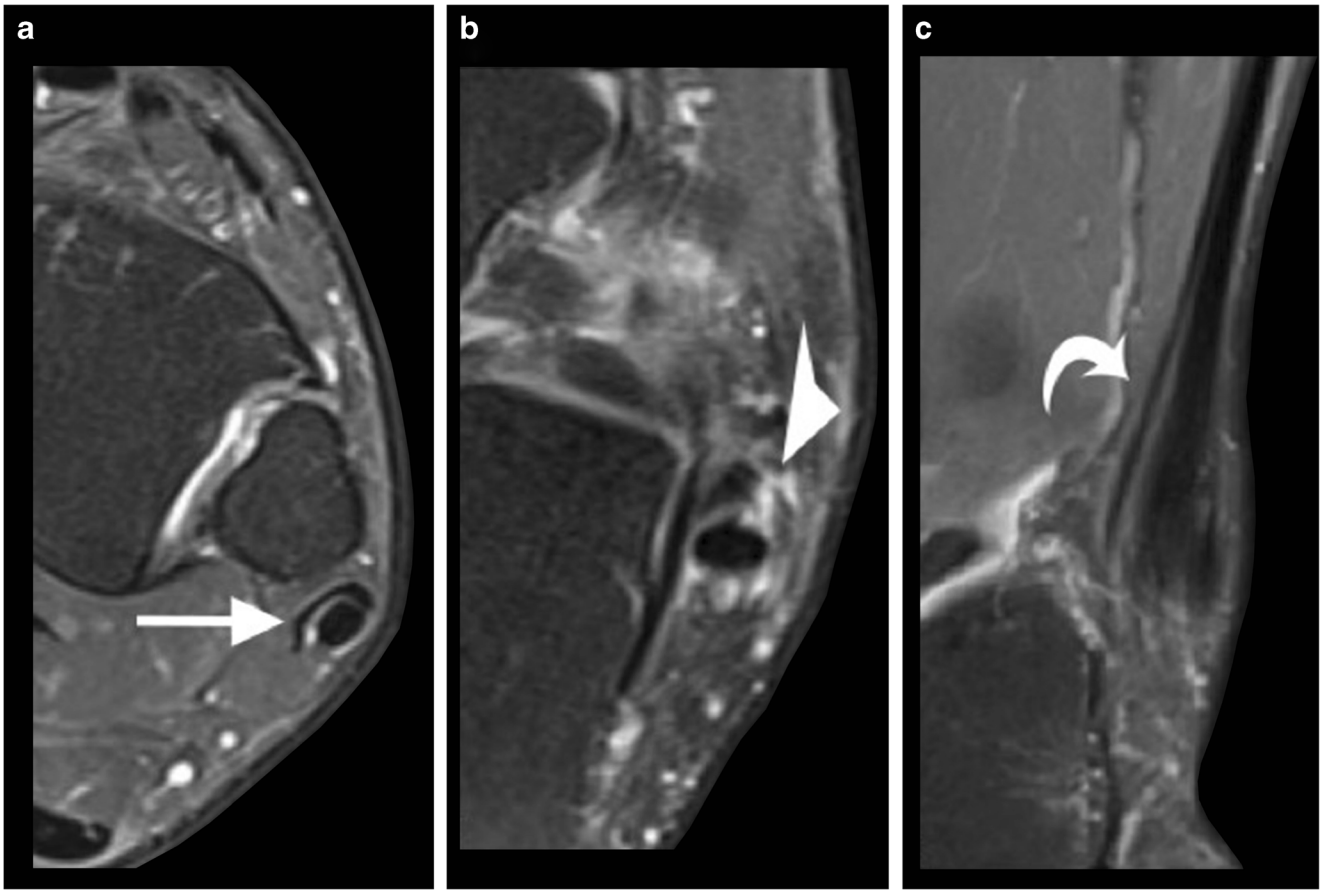

Fig. 5 A 25-year-old-female patient with ankle pain. **a, b** Axial and **c** coronal T2-weighted (T2W) fat-suppressed proton density (PD)-weighted MR images demonstrating the boomerang-shaped PB tendon (*straight arrow*; **a**), longitudinal split tear (*arrowhead*; **b**, and hemitendons (*curved arrow*; **c**) of PB in both sides of the PL tendon

Clinical examination findings

According to the AOFAS scoring system, the mean score was found to be 75.2 ± 18.3. Peroneal tenderness and peroneal instability were observed in 14 (20.3%) and 7 (10.1%) of 69 ankles respectively. In 3 (4.3%) ankles, the patients had both peroneal tenderness and instability. Of these 18 ankles with peroneal tenderness and/or instability, 3 ankles (16.7%) had pathological peroneal tendons on MRI.

Based on the clinical examinations, the sensitivity, specificity, positive predictive value (PPV), and negative predictive value (NPV) of ankle MRIs were found to be 16.6%, 72.5%, 17.6%, and 71% respectively, and the kappa value was 0.579. Based on MRI findings, the sensitivity, specificity, PPV, and NPV of the clinical examinations were 17.6%, 71%, 16.6%, and 72% respectively, and the kappa value was 0.579. We found no relationship between AOFAS scoring values and pathological conditions of the peroneal tendon.

Discussion

Our study demonstrated that the anatomical variations in the lateral ankle presumed to be potentially associated with pathological peroneal tendons are common on ankle MRI. We studied patients with ankle pain, and evaluated the relationship of these variants with patient demographics and pathological conditions of the peroneal tendon.

Retromalleolar groove shape

Galli et al. [2] reported a moderate positive correlation between undulating peroneal grooves and tears of PB tendons. According to some studies, morphological variations in the retromalleolar groove shape, such as flat, convex, or irregular fibular grooves, can predispose individuals to peroneal tendon dislocation and tendon irritation [1, 2]. Although 79.7% of ankles in our study showed one of these shapes, we found no relationship between RMFG shape and pathological peroneal tendons.

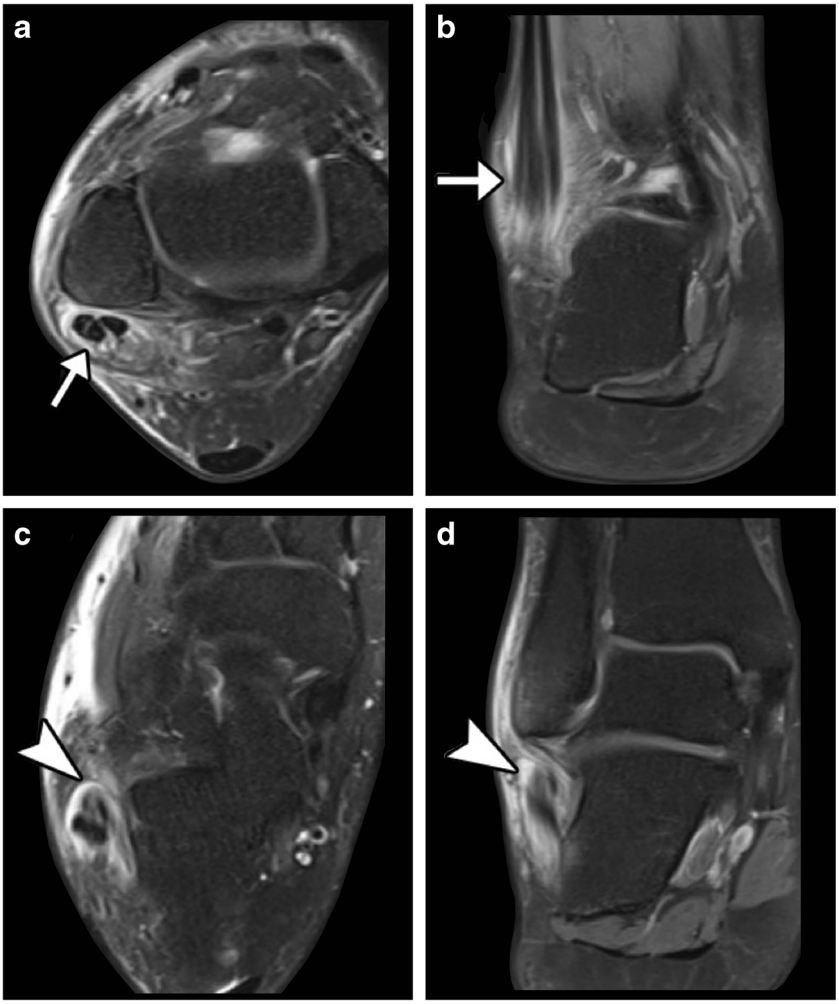

Fig. 6 A 42-year-old male with ankle pain. **a, c** T2W fat-suppressed PD axial **b, d** and coronal MR images demonstrating longitudinal split tears of **a, b** the PL (*straight arrow*) and **c, d** the PB (*arrowhead*) tendons

Peroneal tubercle and retrotrochlear eminence

The first lateral calcaneal prominence was a peroneal tubercle and its prevalence was reported to range from 32% to 100% in the literature [2, 10, 14]. We found that this prominence was very common on ankle MRI with a prevalence of 84%. The second prominence was RTE and we demonstrated it in all ankles (100%) in our study. Similarly, it was reported in 98% and 100% of ankles in the literature [1, 10]. Some studies reported that the sizes of these structures correlated significantly with peroneal tendon disorders. Chronic friction of the PL tendon over the hypertrophic peroneal tubercle is presumed to trigger tendon inflammation and tears [6, 15]. In a study by Saupe et al., the terms "enlarged peroneal tubercle" and "RTE" were defined as measuring more than 5 mm [10]. Although our study revealed hypertrophic peroneal tubercle and RTE in 10% and 32% of ankles respectively, we found no correlation between the sizes of these structures and peroneal pathological conditions.

Low-lying PB muscle belly

A low-lying PB muscle belly is defined as an extension of the muscle tissue distal to the fibular tip. The presence of a low-lying PB muscle belly has been assumed to be one of the risk factors through crowding in the peroneal groove and causing increased SPR laxity and stress placed on the peroneal tendons [2]. In two different studies with asymptomatic ankles, this variation was found in 33% and 38% of patients respectively [2, 10]. Our study revealed this variation in about 23% of ankles. Galli et al. reported a positive weak correlation between low-lying PB muscle bellies and chronic SPR injuries in asymptomatic patients [2]. On the other hand, Mirmiran et al. found a less likely association between low-lying muscle bellies and peroneal tenosynovitis [16]. Our study found no relationship between this variation and SPR injuries or pathological conditions of the peroneal tendon. Although Saupe et al. proposed that extension of the PB muscle belly more than 15 mm distal to the fibular tip should be defined as a low-lying structure, we could not determine a cut-off value

Table 4 Prevalence values of anatomical variants and pathological conditions of the peroneal tendon

Anatomical variants and peroneal tendons	Value (%)
Hypertrophic peroneal tubercle (>5 mm)	7 (10.00)
Hypertrophic retrotrochlear eminence (>5 mm)	22 (32.00)
Low-lying muscle belly	16 (23.20)
Os peroneum	10 (10.00)
Peroneus quartus	9 (13.00)
Peroneocalcaneus externum	8 (89.00)
Peroneoperoneolongus	1 (11.00)
Retromalleolar fibular groove	
Concave	14 (20.30)
Flat	40 (58.00)
Convex	13 (18.80)
Irregular	2 (2.90)
Shape of peroneus brevis tendon	
Anatomical	45 (65.20)
Boomerang	24 (34.80)
Peroneus brevis insertion variation	0
Peroneus longus insertion variation	0
Peroneus brevis tendon	
Intact	54 (78.30)
Tendinosis	7 (10.10)
Partial tear	1 (1.50)
Full-thickness tear	0
Longitudinal split tear	7 (10.10)
Peroneus longus tendon	
Intact	55 (79.70)
Tendinosis	13 (18.80)
Partial tear	0
Full-thickness tear	0
Longitudinal split tear	1 (1.50)

because we could not find a relationship with SPR injuries or pathological peroneal tendons [10]. On the other hand, Rademaker et al. [13] proposed that a dorsiflexed foot position affected the extension of the PB muscle belly. Similar to the study by Saupe et al. [10], we found no correlation between the foot position angle and the location of the PB musculotendinous junction.

Os peroneum

Os peroneum is an accessory bone located within the substance of the PL tendon. It has been presumed to predispose to PL tendon injury because of its location. Anatomical and radiological studies have shown that os peroneum may be present in up to 30% of ankles [2, 17]. Painful os peroneum syndrome has been related to os peroneum fracture, diastasis of multipartite os peroneum, or various pathological conditions of the PL tendon ranging from tenosynovitis to tendon rupture [18]. In our study, os peroneum was found in 13% of ankles, which was bilateral in two patients. There was no bone marrow edema, fracture or multipartite appearance in our ankles. Galli et al. [2] found os peroneum in 10.19% of patients. Although studying asymptomatic patients, they found a moderately positive correlation between os peroneum and pathological PL tendons. Although we studied patients with ankle pain, we found no such correlation. This can be explained by the limited number of patients in our study.

Peroneus quartus muscle

The prevalence of PQ muscle was reported to be between 7% and 22% in previous studies [7, 9, 19]. Similarly, we found this accessory muscle in 13% of ankles. The most common insertion site of the PQ muscle was the calcaneus (peroneocalcaneus externum muscle), which was seen in 89% of our ankles. In 11% of ankles, it inserted at the PL tendon (peroneoperoneolongus muscle). We found no cuboid bone insertions. Our results were in agreement with the studies by Saupe et al. and Cheung et al. in which the reported percentages of calcaneal insertions were 91% and 79% respectively [10, 20]. In the literature, PQ muscles was found more frequently in male patients [9, 10, 20]. In contrast, our study revealed this variation to be more common in women; however, we found no statistically significant relationship with sex. It was assumed that the presence of the PQ muscle could predispose to dislocation and tear of the PB tendon through crowding in the retromalleolar groove [1, 7, 9]. However, we found no significant correlation between the presence of PQ muscles and pathological conditions of the PB tendon.

Peroneal tendon variations and pathological conditions

The PB tendon is situated anteromedial to the PL tendon and normally has a flat or mildly crescentic shape. If the PB tendon has a boomerang-shape with central thinning and degeneration, it has been proposed to be a risk factor for tears of both the PB and the PL tendon. In our study, boomerang-shaped PB tendons were found in 34.8% of ankles and more commonly in female patients. Galli et al. reported a statistically significant correlation between boomerang-shaped PB tendons and both PB and PL tendinopathies [2]. We also found significant correlations between boomerang-shaped PB tendons and pathological features of both PB and PL tendons.

The normal insertion sites of the peroneal tendons are on the lateral aspect of the fifth metatarsal base for PB tendons, and on the plantar posterolateral aspect of the medial cuneiform and the lateral side of the first metatarsal base for PL tendons. Cecava and Campbell reported variant congenital insertion of the peroneus brevis tendon on the calcaneal

Table 5 Correlations among anatomical variants, additional pathological findings, and pathological conditions of the peroneal tendon

	Peroneus brevis Tendinosis	Peroneus brevis Tear	Peroneus longus Tear/tendinosis
Boomerang-shaped peroneus brevis tendon	0.002*	0.006*	0.014*
Soft-tissue edema	0.087	0.004*	0.028*

Data are presented as correlation coefficients

*Correlation statistically significant at $p \leq .05$

peroneal tubercle in up to 1% of the population [21]. No insertional variations of peroneal tendons were found in our study.

We found tendinosis in 10.1% and 18.8% of PB and PL tendons respectively. There were no complete tears of PB or PL tendons, and only one ankle (1.5%) with a partial tear of the PB tendon in our study. Although longitudinal split tears of the PB have been reported to be more common in the surgical literature, its occurrence in the PL tendon is less common. The most likely proposed mechanisms for longitudinal split tears of peroneal tendons are mechanical, such as SPR disruption, shallow fibular groove, low-lying PB muscle belly, and the presence of the PQ muscle, which may cause tendon dislocation [22]. Although there were no MRI findings of peroneal tendon dislocation, we showed longitudinal split tears of PB and PL tendons in 7 (10.1%) ankles and 1 (1.5%) ankle respectively. Longitudinal split tears of both PB and PL tendons were demonstrated in a female patient. No significant correlations were found between peroneal pathological conditions and age or sex. Similar to the study by Galli et al. [2], we found a significant correlation between boomerang-shaped PB tendons and peroneal tendinopathies (tendinosis and tears of PB and PL tendons). As mentioned previously, no other ankle variations showed any relationship with pathological conditions of the peroneal tendon.

Additional pathological conditions of the lateral ankle on MRI

The SPR forms the posterolateral border of the fibular groove and retains the peroneal tendons in this fibro-osseous tunnel. It is a widely accepted that SPR injuries are often associated with subluxation or dislocation of peroneal tendons, which are major predisposing factors for peroneal tendon tears. Although we found no positive correlation between SPR injuries and peroneal tendon disorders, this could be explained by the limited number of patients (8.7%) in our study.

Lateral ankle soft-tissue edema is a common finding on ankle MRI; it was present in 42% of our ankle MR examinations. There was a significant correlation between this finding and pathological conditions of both the PB and the PL tendon. We noted synovial effusion and thickening of peroneal tendon sheaths in 34.8% and 10.1% of ankle MR examinations respectively. We found no correlation between synovial findings and peroneal tendinopathies. The finding of synovial effusion is not specific to pathological conditions of the peroneal tendon and its presence is not uncommon on ankle MRI in both asymptomatic and symptomatic patients in daily routine.

Clinical examination findings

We found peroneal tenderness and instability in 20.3% and 10.1% of ankles respectively. Of the ankles with peroneal tenderness and/or instability, only 16.7% of ankles had a pathological peroneal tendon on MRI. Our study demonstrated a poor correlation between clinical and MRI findings, with the low sensitivity (17.6%) and PPV (16.6%) values of clinical findings compared with MRI results for pathological conditions of the peroneal tendon. Similarly, O'Neil et al. reported pathological peroneal tendons on MRI in 103 out of 294 asymptomatic patients (35%) [12]. These results suggest that pathological conditions of the peroneal tendon are often incidental findings on ankle MRI regardless of the clinical symptoms. Additionally, there was no correlation between AOFAS values and pathological peroneal tendons on MRI in our study.

Our study showed that MRI had very low sensitivity (16.6%) and PPV (17.6%) values for pathological peroneal tendons. Similarly, the studies by Giza et al. [23] and Kuwada [24] reported low PPV (48%) and sensitivity (57%) values of MRI for peroneal tendon tears respectively. In another study by Park et al., the surgical and preoperative MRI findings were compared in 97 patients with lateral ankle symptoms. Similarly, they reported low sensitivity of MRI for interstitial tears of PB and PL tendons, which were 44% and 50% respectively [25].

There were some limitations in our study. The most important restriction was the limited number of patients in our study. The second limitation was that both 1.5-T and 3 T-MR systems were used in the study. We used a head coil in the 3-T system because there was no extremity coil. To prevent technical heterogeneity between these devices, we used pillows around the ankle in both the extremity and head coils for a standard position, with a 90° angle between the leg and the foot. We also used similar sequence parameters in both devices. As the last limitation, albeit minor, our study population included more women than men. Although we found no relationships between anatomical variations and sex except for the RMFG shape and os peroneum, these relationships should be evaluated in a larger patient group with similar numbers of women and men.

Conclusion

Anatomical variations are common on ankle MRI and cannot be considered a major risk factor in pathological conditions of the peroneal tendon, except for boomerang-shaped PB tendons, according to our study. Both MRI and clinical examinations have low sensitivity in the diagnosis of pathological peroneal tendons and they are often incidental findings on MRI. Although our study has the advantage of including symptomatic patients and the use of a standard clinical scoring system, further prospective and long-term studies with larger populations, including both symptomatic and asymptomatic patients, should be performed to establish a causal relationship.

Compliance with ethical standards

Conflicts of interest The authors declare that they have no conflicts of interest.

Publisher's note Springer Nature remains neutral with regard to jurisdictional claims in published maps and institutional affiliations.

References

1. Wang XT, Rosenberg ZS, Mechlin MB, Schweitzer ME. Normal variants and diseases of the peroneal tendons and superior peroneal retinaculum: MR imaging features. Radiographics. 2005;25:587–602.
2. Galli MM, Protzman NM, Mandelker EM, Malhotra AD, Schwartz E, Brigido SA. An examination of anatomic variants and incidental peroneal tendon pathologic features: a comprehensive MRI review of asymptomatic lateral ankles. J Foot Ankle Surg. 2015;54:164–72.
3. Hammerschlag WA, Goldner JL. Chronic peroneal tendon subluxation produced by an anomalous peroneus brevis: case report and literature review. Foot Ankle. 1989;10:45–7.
4. Geller J, Lin S, Cordas D, Vieira P. Relationship of a low-lying muscle belly to tears of the peroneus brevis tendon. Am J Orthop (Belle Mead NJ). 2003;32:541–4.
5. Buschmann WR, Cheung Y, Jahss MH. Magnetic resonance imaging of anomalous leg muscles: accessory soleus, peroneus quartus and the flexor digitorum longus accessorius. Foot Ankle. 1991;12:109–16.
6. Boles MA, Lomasney LM, Demos TC, Sage RA. Enlarged peroneal process with peroneus longus tendon entrapment. Skeletal Radiol. 1997;26:313–5.
7. Zammit J, Singh D. The peroneus quartus muscle: anatomy and clinical relevance. J Bone Joint Surg Br. 2003;85:1134–7.
8. Rosenberg ZS, Bencardino J, Astion D, Schweitzer ME, Rokito A, Sheskier S. MRI features of chronic injuries of the superior peroneal retinaculum. AJR Am J Roentgenol. 2003;181:1551–7.
9. Sobel M, Levy ME, Bohne WH. Congenital variations of the peroneus quartus muscle: an anatomic study. Foot Ankle. 1990;11:81–9.
10. Saupe N, Mengiardi B, Pfirrmann CW, Vienne P, Seifert B, Zanetti M. Anatomic variants associated with peroneal tendon disorders: MR imaging findings in volunteers with asymptomatic ankles. Radiology. 2007;242:509–17.
11. Saxena A, Luhadiya A, Ewen B, Goumas C. Magnetic resonance imaging and incidental findings of lateral ankle pathologic features with asymptomatic ankles. J Foot Ankle Surg. 2011;50:413–5.
12. O'Neil JT, Pedowitz D, Kerbel YE, Codding JL, Zoga AC, Raikin SM. Peroneal tendon abnormalities on routine magnetic resonance imaging of the foot and ankle. Foot Ankle Int. 2016;37(7):743–7.
13. Rademaker J, Rosenberg ZS, Beltran J, Colon E. Alterations in the distal extension of the musculus peroneus brevis with foot movement. AJR Am J Roentgenol. 1997;168:787–9.
14. Agarwal AK, Jeyasingh P, Gupta SC, Gupta CD, Sahai A. Peroneal tubercle and its variations in the Indian calcanei. Anat Anz. 1984;156:241–4.
15. Hyer CF, Dawson JM, Philbin TM, et al. The peroneal tubercle: description, classification, and relevance to peroneus longus tendon pathology. Foot Ankle Int. 2005;26:947–50.
16. Mirmiran R, Squire C, Wassell D. The prevalence and role of low lying peroneus brevis muscle belly in patients with peroneal tendon pathologies: a potential source for tendon subluxation. J Foot Ankle Surg. 2015;54(5):872–5.
17. Muehleman C, Williams J, Bareither ML. A radiologic and histologic study of the os peroneum: prevalence, morphology, and relationship to degenerative joint disease of the foot and ankle in a cadaveric sample. Clin Anat. 2009;22(6):747–54.
18. Sobel M, Pavlov H, Geppert MJ, Thompson FM, DiCarlo EF, Davis WH. Painful os peroneum syndrome: a spectrum of conditions responsible for plantar lateral foot pain. Foot Ankle Int. 1994;15(3):112–24.
19. Cheung Y, Rosenberg ZS. MR imaging of the accessory muscles around the ankle. Magn Reson Imaging Clin N Am. 2001;9:465–73.
20. Cheung YY, Rosenberg ZS, Ramsinghani R, Beltran J, Jahss MH. Peroneus quartus muscle: MR imaging features. Radiology. 1997;202:745–50.
21. Cecava ND, Campbell SE. Peroneus brevis tendon variant insertion on the calcaneus. J Radiol Case Rep. 2015;9(5):22–9.
22. Diaz GC, van Holsbeeck M, Jacobson JA. Longitudinal split of the peroneus longus and peroneus brevis tendons with disruption of the superior peroneal retinaculum. J Ultrasound Med. 1998;17(8):525–9.
23. Giza E, Mak W, Wong SE, Roper G. A clinical and radiological study of peroneal tendon pathology. Foot Ankle Spec. 2013;6(6):417–21.
24. Kuwada GT. Surgical correlation of preoperative MRI findings of trauma to tendons and ligaments of the foot and ankle. J Am Podiatr Med Assoc. 2008;98:370–3.
25. Park HJ, Lee SY, Park NH, et al. Accuracy of MR findings in characterizing peroneal tendon disorders in comparison with surgery. Acta Radiol. 2012;53:795–801.